Metal halide perovskite solar module encapsulation using polyolefin elastomers: the role of morphology in preventing delamination

Haoyang Jiao¹, Maruti Hegde¹, Nengxu Li¹, Michael Owen-Bellini³, Laura Schelhas³, Theo J. Dingemans¹, Jinsong Huang^{1,2}

¹Department of Applied Physical Sciences, the University of North Carolina at Chapel Hill,

Chapel Hill, NC, 27599, USA.

²Department of Chemistry, the University of North Carolina at Chapel Hill, Chapel Hill, NC, 27599, USA.

³National Renewable Energy Laboratory, Golden, CO, 80401, USA.

KEYWORDS: encapsulant, polyolefin elastomers, perovskite, solar cells, delamination

ABSTRACT: The development of perovskite solar cells (PSCs) has ushered in a new era of solar technology, characterized by its exceptional efficiency and cost-effective production. However, the soft and fragile nature of perovskites makes module encapsulation challenging. Polyolefin elastomers (POEs) have been reported to be promising encapsulants for perovskite modules. However, little research exists on identifying criteria among different types of POEs as

encapsulants. Here, two POEs with different morphologies were compared as encapsulants. The first POE crystallizes during encapsulation (crystal content ~40%), and the resulting shrinkage/warpage leads to delamination causing minimodule failure. In contrast, perovskite minimodules encapsulated with a mostly amorphous POE exhibited better reliability, reproducibility. The best perovskite minimodules passed the thermal cycling (TC) for 240 cycles between -40 C to 85 C, and damp heat (DH) test for 1419 hours according to IEC 61215 standard. This study highlights the importance of morphology of encapsulants in achieving high quality encapsulation.

Popular summary: The perovskite solar cells (PSCs) are at the forefront of solar technology innovation, offering a promising pathway to highly efficient and cost-effective renewable energy. However, the soft and fragile nature of metal halide perovskite makes module encapsulation challenging. This work focused on the impact of polyolefin elastomers morphology as encapsulants on the protection and durability of PSCs. We compared two commercial POEs: one crystallizes and resulting shrinkage causes module failure, while an amorphous POE enhances minimodule reliability, passing the rigorous thermal cycling and damp heat tests. This work highlights the critical role of encapsulant morphology in extending the lifespan of perovskite modules, guiding future material selection for PSCs encapsulation.

Introduction.

Perovskite solar cells (PSCs) have demonstrated rapid improvement in power conversion efficiency attaining 26.1% for single junction cells and 33.9% for monolithic perovskite/silicon tandem cells.^[1] Despite performance advancements, perovskite photovoltaics (PV), particularly modules, continue to face long-term durability issues, which remains the most significant hurdle

to commercialization. In addition to the intrinsic stability of perovskites, encapsulation technology is critical to the module's longevity^[2,3]. The encapsulation serves as a protection against environmental factors such as moisture and oxygen and thus should have low permeability to them.

[4-9] In addition, the encapsulating materials themselves also need to have an appropriate modulus in order to avoid stress-related damage^[10], should be processable under conditions that does not damage the perovskite solar modules during production^[11–14], and must remain stable during 25-30 years operation in field.

Glass-glass lamination technology—adapted from Si and CdTe solar cell encapsulation that incorporates various polymer encapsulants and edge sealants are widely used to encapsulate PSCs. Compared with Si and CdTe, perovskites are more temperature sensitive and softer, therefore the encapsulants need to provide mechanical protection without introducing stress and can be laminated at relatively low temperature. Among the diverse polymeric materials evaluated, including ethyl vinyl acetate (EVA)^[10,15–21], poly isobutylene (PIB)^[22,23], polyolefin elastomer (POE)^[10,16,24], Surlyn^[10,15], and thermoplastic polyurethane (TPU)^[16,25], each demonstrated specific advantages and limitations. Notably, EVA's high encapsulation temperature (>140 °C) and acid byproducts during aging were detrimental to perovskite device stability.^[26,27] Surlyn films, despite their superior reliability, were prone to delamination issues due to their high tensile modulus. [10] Preliminary evaluation of TPU demonstrated its commendable performance in certain scenarios, while it is relatively expensive^[28].Polyolefin elastomers (POEs) have emerged as one of the most extensively researched encapsulants. [10,16,24,28]. POE exhibits low water vapor transmission rates (WVTR) (~0.8 g/m² day), sufficient thermal stability (degradation occurs above 300 °C), optical transparency (~91%)^[29], and can be processed at temperatures and pressures that does not damage most of perovskites for solar cells. Moreover, POEs are relatively low-cost

compared to other polymers suitable as encapsulants. POEs are typically copolymers obtained by metallocene polymerization of ethylene-based monomers along with other alpha-olefin monomers. By tuning monomer structures and monomer functionality, polymer backbone structures/architectures, and hence their thermomechanical and morphological properties can be easily altered. Despite widespread use as an encapsulant material by research groups, research has not yet fully explored what POE properties are required to act as an encapsulant for perovskite solar cells.

Herein, we compare PSC performance using two POEs as encapsulating materials. One of them, referred to as POE-1, is commercially available from DNPsolar, a subsidiary of Dai Nippon Printing Co., Ltd., Japan. The second POE used for comparison, POE-2, is an experimental grade material. The morphological characteristics, thermal, and thermo-mechanical behaviors of POE-1 and POE-2 were studied and used to rationalize device performance, stability following encapsulation. Specifically, the performance and durability of minimodules with the two POEs were evaluated using accelerated stress tests (thermal cycling and damp heat) in accordance with the International Electrotechnical Commission (IEC) 61215-2:2021 module qualification tests^[30]. Our work demonstrates that amorphous POEs and POEs with a low degree of crystallinity result in better encapsulation for PSCs.

Results and Discussions.

A schematic diagram of the components of an encapsulated minimodule is shown in Figure 1a^[29]. In our typical minimodule encapsulation procedure, desiccated polyisobutylene (PIB) edge sealant was adhered to the edges of ITO glass and cover glass and worked as moisture barrier^[19]. The SnPb solder coated copper ribbons (shown as rods in **Figure 1a**) were placed in between two

PIB sealants to minimize moisture penetration. Two encapsulant (POE-1 or POE-2) films were placed between the cover glass and the device to reduce the thickness mismatch between PIB and POE encapsulant films. This whole assembly was then placed in a laminator for encapsulation. The optimal pressure and temperature conditions were determined based on characterization of both POEs. The detailed encapsulation method is provided in the experimental section.

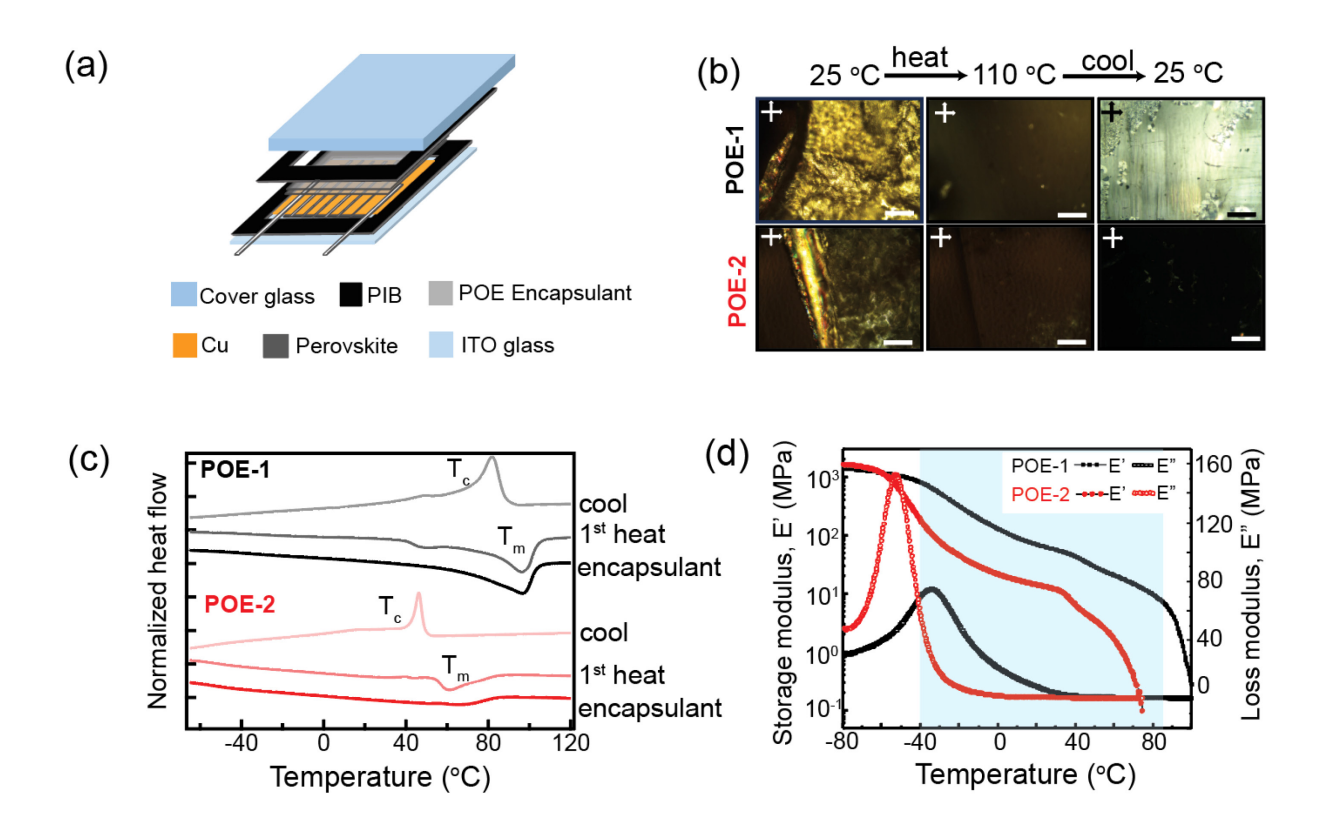


Figure 1. PSC minimodule and POE characterization. (a) Schematic illustration of the minimodule encapsulation components. (b) Morphological changes that occur when POE-1 and POE-2 films are heated and cooled between crossed polarizers of an optical microscope. The temperatures are mentioned above the images. The scale bar in all images is 200 μm. Upon cooling, only POE-1 appears highly birefringent (high crystal content) whereas POE-2 is weakly birefringent (low crystal content). (c) DSC curves for POE-1 and POE-2 films subjected to a heat-

cool cycle. Curves were vertically translated for clarity. Analysis (heating curve) of POE films subjected to minimodule encapsulation processing conditions confirms similar thermal transitions as the 1st heat curves. (d) Storage (E') and loss modulus (E") curves obtained at 1 Hz, tensile mode as a function of temperature for POE-1 and POE-2 films. The higher crystallinity in POE-1 films results in larger E' values above T_g. The blue shaded box covers the temperature range that POE encapsulants experience during thermal cycling.

Scanning thermogravimetric analysis (TGA) of the two polymers (10 °C/min) revealed onset of thermal decomposition temperature at 385 °C for both POEs (Figure S1, Supplementary **Information (SI)** which is higher than the operational temperature range of the perovskite solar minimodules. Heating and cooling the films on a hot-stage between crossed polarizers of an optical microscope enabled visualization of the morphological changes that occur in POE films during (Figure 1b) minimodule encapsulation. The observed birefringence at 25 °C due to a semicrystalline morphology disappears upon complete melting at 110 °C. Upon complete melting and cooling, only POE-1 appears highly birefringent, i.e. POE-1 was able to recrystallize during the cooling process (Figure 1b, top row) whereas POE-2 stayed mostly amorphous with few, scattered crystallites (Figure 1b, bottom row). Additionally, the melt viscosity at 110 °C was qualitatively judged to be low enough for processing of POEs during encapsulation. The observations from crossed polarized optical microscopy were quantitatively analyzed using differential scanning calorimetry (DSC) (**Figure 1c**). POE-1 exhibits a weak glass transition (T_g) that is centered at -31 °C followed by a large, broad melt endotherm (T_m) (between 39 °C to 120 °C), with a melt enthalpy (ΔH_f) of ~90 J/g. The subsequent cooling curve reveals a large exotherm due to

crystallization (T_c) with an identical ΔH of ~90 J/g. In contrast, POE-2 exhibits a lower T_g (-51 °C), with a smaller T_m peak with $\Delta H = \sim 19 \text{ J/g}$ and crystallization upon cooling (ΔH of 19 J/g). A rough estimate of relative crystallinity value (χ_c) based on polyethylene ($\chi_{100\%} = 293$ J/g) and polypropylene ($\chi_{100\%} = 207 \text{ J/g}$) indicates χ_c for POE-1 lies between 31% and 44% whereas χ_c for POE-2 is between 6% - 9%^[31]. These results demonstrate that POE-1 has a greater propensity to crystallize than POE-2. Thermo-mechanical analysis was performed on both POE films using dynamic mechanical thermal analysis (DMTA) (**Figure 1d**). At -80 °C, both films exist in a glassy state, and their stress-response is dominated by the elastic component i.e. high E' and low E", resulting in typical glassy E' values (~1600 MPa for both POEs). Upon increasing the temperature, the polymers soften at the T_g and E^{\prime} decreases dramatically. Concurrently, the $E^{\prime\prime}$ exhibits a peak at -52 °C and -33 °C, signifying molecular dissipative transitions i.e. the T_{g} wherein viscoelastic behavior dominates. Although both POE-1 and POE-2 exhibit a clear rubbery plateau between 0 °C to 35 °C before onset of melt, the E' for POE-1 is much higher than POE-2 (at 30 °C, E' = 62 MPa and 9 MPa for POE-1 and POE-2 respectively). The larger E' in the rubbery plateau region of POE-1 arises from the higher crystal content i.e. the crystal domains act as physical crosslinking sites for the amorphous polymer chains thereby limiting their deformation. The E' drops dramatically again (onset at 45 °C for POE-1 and 35 °C for POE-2) due to crystalline melting. The mechanical properties (Young's modulus and strength) from stress-strain measurements at 25 °C (Figure S2) confirms that higher crystal content in POE-1 makes it stiffer and stronger than POE-2 above T_g .

The contrasting crystallizability of POE-1 and POE-2 impacts device encapsulation. To visualize the effect of crystallization on dimensional stability of POE films, POE films on a BynelTM support were subjected to the processing temperature (110 °C for 10 min) used for

encapsulation followed by slow, natural cooling to 25 °C. The propensity of POE-1 to crystallize significantly (between 31-44%) while cooling results in extensive film warping due to crystallization induced dimensional change (warpage, shrinkage)[32] and delaminate from the BynelTM support at the edges (Figure 2a). In contrast, such extensive warpage is not observed in predominantly amorphous POE-2 films (Figure 2b). POE-2 films on a BynelTM support remain adhered with minimal warpage due to lack of crystallization during cooling. The estimated inward curvatures (Figure S3) for POE-1 are 0.75 cm and 2.02 cm for POE-2. A stack to mimic the minimodule was constructed by laminating PIB and POE between two glass covers and then subjected to the encapsulation processing conditions (Figure S4). The stack with POE-1 films exhibits thickness variation (5.20 mm in the center and 5.14 mm at the edge) throughout the sample due to dimensional changes (warpage, shrinkage). In contrast, the stack formed using POE-2 shows minimal thickness variations (5.36 mm in the center and 5.34 mm at the edge). The solar cell minimodules used in this work is composed of ITO/Poly[bis(4-phenyl)(2,4,6-trimethylphenyl) (PTAA)/ FA_{0.9}Cs_{0.1}PbI₃/ C₆₀/Bathocuproine(BCP)/Cu. In minimodules, crystallinity induced dimensional changes in POE-1 causes delamination at the edges on both Cu-side and ITOside whereas no such issues were observed in POE-2 encapsulated minimodules (Figure 2c, Figure 2d). The schematics shown in Figure 2e and Figure 2f helps visualize the mechanism by which the delamination occurs.

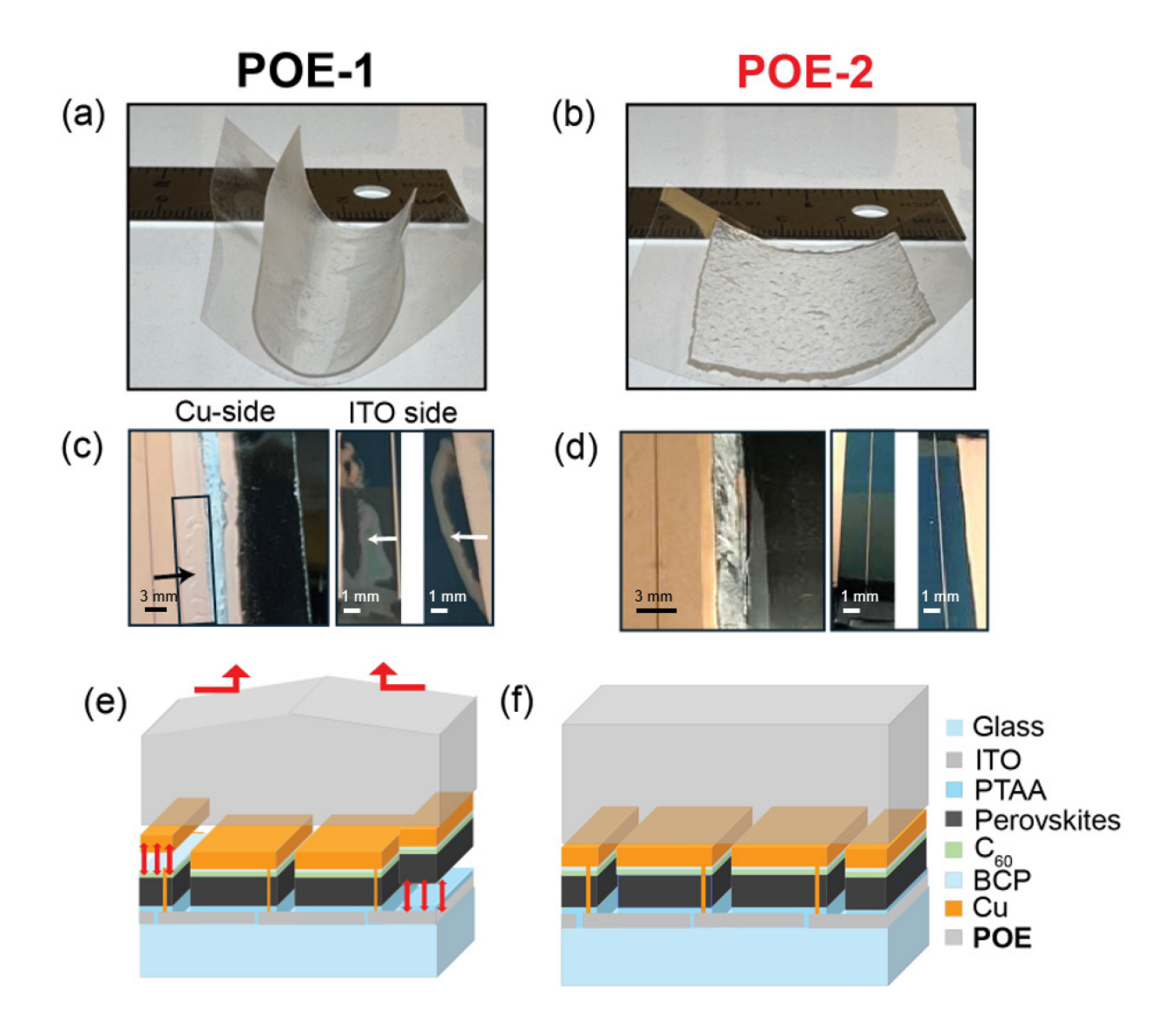


Figure 2. Analysis of minimodules encapsulated with POE-1 and POE-2. (a) POE-1 with BynelTM support after cooling down with warpage and delamination from the BynelTM support at the edge. (b) POE-2 with BynelTM support after cooling down remaining adheared with minimal warpage. (c) PSC minimodules encapsulated with POE-1, delamination of encapsulants from the device is observed predominantly at the edges on the Cu-side and ITO side. The arrows point to delaminated sites. (d) PSC minimodules encapsulated with POE-1 No delamination is observed in devices encapsulated with POE-2. (e) A schematic of POE-1 encapsulated minimodule showing

the warping of POE-1 that causes delamination of Cu from perovskite and perovskite from HTL.

(f) A schematic of a POE-2 encapsulated minimodule without delamination issues is shown for comparison.

Photoluminescence (PL) and electroluminescence (EL) mapping of the minimodules before and after encapsulation with POE-1 and POE-2 were performed to understand how minimodule performance was impacted by encapsulation (**Figure 3**). We selected two minimodules with minimal visible delamination and optimal PCEs for this study.

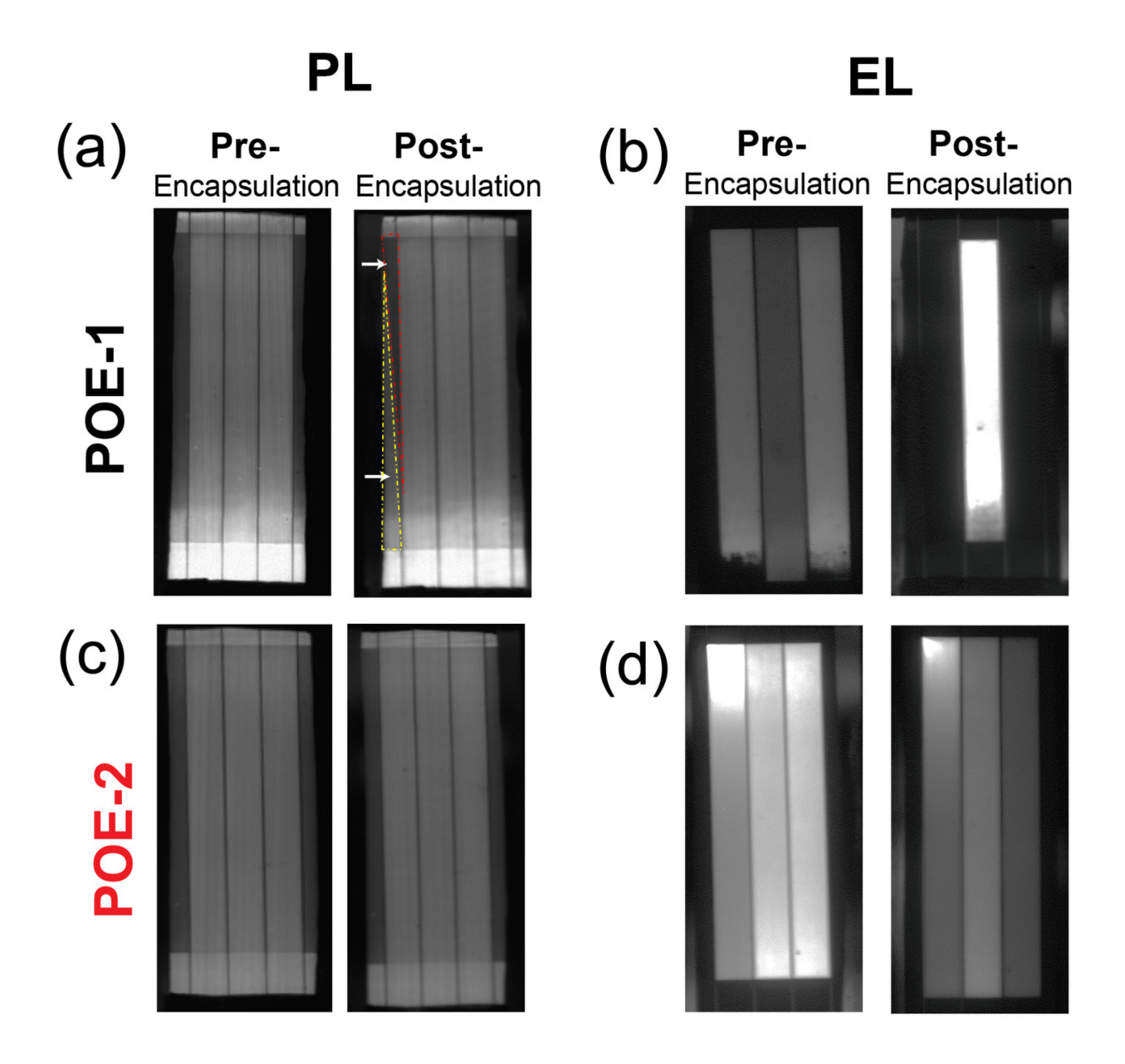


Figure 3. Photoluminescence (PL) and electroluminescence (EL) mapping of minimodules pre- and post-encapsulation with POE-1 and POE-2. (a) PL of POE-1 based minimodule pre- and post-encapsulation. (b) EL of POE-1 based minimodules pre- and post-encapsulation. EL signals from both edges disappear post-encapsulation. (c) PL of POE-2 based minimodules pre- and post-encapsulation. (d) EL of POE-2 based minimodules pre- and post-encapsulation.

The results shown in **Figure 3** are consistent with our findings shown in **Figure 2**. The left edge of the minimodule post-encapsulation (red and yellow frame areas marked by arrows) exhibited a clear contrast, indicating damage to the perovskite layer which is caused by POE-1 delamination. (Figure 3a). Additionally, we measured the minimodule EL with a constant injected 3 mA current which is about 5% of the minimodule short-circuit current to minimize the possible damage of minimodules by forward current. We observed the disappearance of edge EL signals (Figure 3b) on POE-1 encapsulated minimodule post encapsulation. The input voltage of the minimodule during EL measurement dropped from 2.76 V (pre-encapsulation) to 1.62 V (post encapsulation) which indicates the minimodule is partially short circuited or shunted at the P3 area due to the POE-1 warpage/shrinkage at the edge (Figure 2e and Figure S4). In minimodules encapsulated using POE-2, there is negligible difference in PL intensities compared to the pre-encapsulated minimodules (Figure 3c) which means no damage to the perovskite occurred during the encapsulation process. The minimodule encapsulated with POE-2 demonstrates only slight change in EL mapping intensities, and the measured voltage of the minimodule during EL had a slight change from 3.41 V (pre-encapsulation) to 3.43 V (post encapsulation) which indicates no big contact resistance change during the encapsulation, implying superior encapsulation quality.

The PCE change before and after lamination for both POE-1 and POE-2 encapsulated minimodules with an aperture area between 9.9 to 17.9 cm² are shown in **Figures S5-S7**. Since most minimodules encapsulated with POE-1 experienced delamination issues, leading to failure after lamination, only 2 out of 8 minimodules survived with reduced Voc, J_{SC} and FF after lamination (**Table S1 and S2**), the survived minimodules PCE were shown in **Figure S5**. One of the minimodules FF reduced from 62% to 58% which reduced the PCE by 4.8% post encapsulation. The Voc of the other surviving minimodule dropped by 25.0%, I_{SC} dropped by 12.4% and the FF

dropped by 9.5% which reduced the PCE by 40% post encapsulation. Conversely, POE-2 encapsulated minimodules demonstrated increased V_{OC} and FF, thereby enhanced PCE (**Figure S6**). Statistical data for the performance of POE-2 encapsulated minimodules pre- and post-encapsulation is shown in **Figure S7**. Totally, all the ten tested modules survived after the POE-2 encapsulation and the detailed parameters are listed in **Table S3** and **S4**. On average, the minimodules V_{OC} increased by 2.3%, I_{SC} increased by 1.4%, FF increased by 9.3% and the PCE increased by 12.1% post encapsulation.

Encapsulated minimodules were subjected to thermal cycling and damp heat tests. The thermal cycling test adheres to IEC 61215 standards (200 cycles, temperature limits of -40 °C and 85 °C) and the damp heat test was performed at 85 °C \pm 2 °C at a relative humidity of 85%. While these tests do not offer a direct prediction of the device long-term stability in field test, they help identify reasons behind failures in the device packaging.

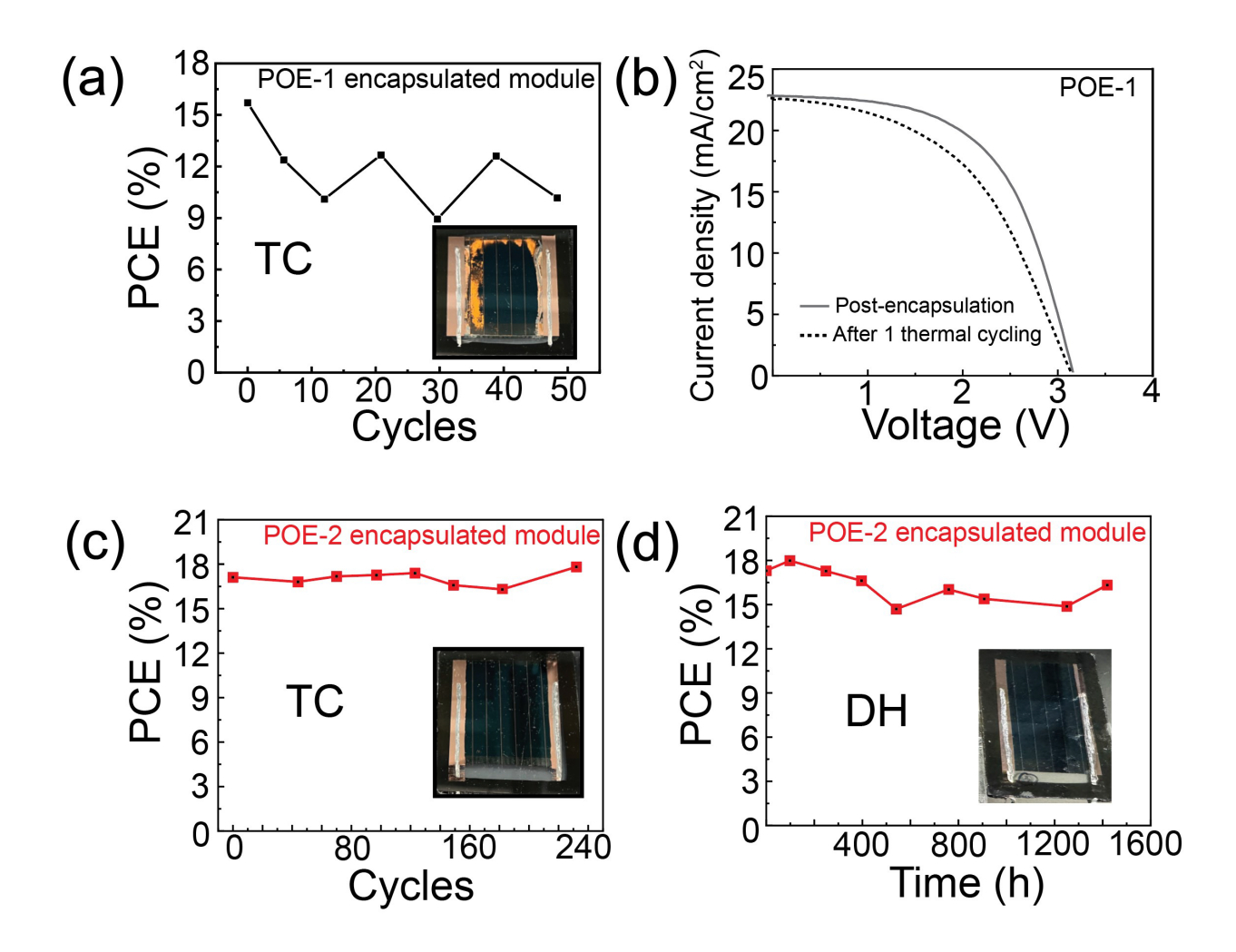


Figure 4 Durability assessments of POE-1 and POE-2 encapsulated minimodules. (a) PCE change of a POE-1 encapsulated minimodule during thermal cycling test with the final picture of the minimodule, showing the degradation of the edge perovskite. (b) J-V curves of a POE-1 encapsulated minimodule after encapsulation and one thermal cycle. (c) PCE change of POE-2 encapsulated minimodule during thermal cycling test with the final picture of the minimodule, showing no obvious degradation. (d) PCE evolution of POE-2 encapsulated minimodule during damp heat test with the final picture of the minimodule, showing no obvious degradation.

POE-1 encapsulated minimodules didn't pass the thermal cycling test and the edge of the minimodule showed obvious degradation (**Figure 4a**). In fact, the PCE of the best POE-1 encapsulated minimodule decreased by 20% of its initial PCE after only one temperature cycle (**Figure 4b**). The detailed parameters are listed in **Table S5**. Due to the failure of the POE-1 encapsulated minimodules in the thermal cycling test, they were not subjected to the subsequent damp heat testing. The best POE-2 encapsulated minimodule maintained 100 % of its highest PCE after 240 thermal cycles (**Figure 4c**). The evolutions of V_{OC}, J_{SC}, FF and PCE for this device are summarized in **Figure S8**. During thermal cycling, the temperature was changed between -40 °C and 85 °C wherein the E' varies between 181 MPa and 0.1 MPa, respectively (**Figure 1d**). Despite this large change of stiffness, no delamination was observed during thermal cycling. Additionally, the best POE-2 encapsulated minimodule demonstrated exceptional durability, retaining 90.7% of its highest PCE after 1419 hours of damp heat test (**Figure 4d**). The evolutions of V_{OC}, J_{SC}, FF and PCE for this device are summarized in **Figure S9**.

Conclusions.

The morphological, thermal and thermo-mechanical characterization of two polyolefin elastomers with different crystallinity enabled determination of how encapsulant morphology could impact PSC minimodule encapsulation. During PSC minimodule encapsulation using a highly crystallizable polymer (χ_c is between 31-44%), crystallization induced warpage/shrinkage of POE-1 caused delamination and minimodule failure. In contrast, minimodules encapsulated with POE-2 that remained mostly amorphous (χ_c is only 6-9%) not only passed the thermal cycling and damp heat test, but also improved minimodule PCE by the encapsulation. It is not clear yet why the solar cell efficiency enhanced after encapsulation. Additionally, during thermal cycling,

no delamination was observed despite of the dramatic changes in POE -2 stiffness; E' ranges from 181 MPa (-40 °C) to 0.1 MPa (85 °C). Our work provides crucial insights for guiding encapsulant selection for enhanced minimodule stability and performance.

Supplemental Material

See Supplemental Material at [] for detailed materials^[33], device fabrication, device encapsulation procedures, descriptions of analysis techniques: stress-strain measurements, dynamic mechanical thermal analysis measurements, thermogravimetric analysis, differential scanning calorimetry, cross-polarized optical microscopy, photoluminescence mapping and electron luminescence mapping measurements.

Acknowledgements. This work is mainly supported by National Science Foundation under award DMR-1903981 and Office of Naval Research under award N6833522C0122. LTS was supported by the U.S. Department of Energy Office of Energy Efficiency and Renewable Energy (EERE) under the Solar Energy Technologies Office (SETO) "Advanced Perovskite Solar Cells and Modules" program (Agreement Number 38256).

Author Contribution: H.J. and J.H conceived the idea and designed the experiments. H.J. and M.O. conducted the encapsulation optimization. H.J. conducted device characterizations and stability measurement. H.J. and N.L. fabricated the perovskite minimodules. H.M. conducted the characterizations of the POEs. H.J., M.H and T.D. conducted the POEs property analysis. H.J.,

M.H. and J.H. wrote the paper, and all the authors reviewed the paper. H.J. and M.H. contribute equally to this paper.

Competing interests: Huang, J. disclose the following financial conflict of interest. Tandem PV is an entity to which the following technologies used or evaluated in this paper have been licensed: an ink formulation for fast coating of perovskites and BHC for reducing iodine. Huang is an inventor of the technologies and has received royalties. These relationships have been disclosed to and are under management by UNC-Chapel Hill. The remaining authors declare no competing interests.

References

- (1) Best Research-Cell Efficiency Chart. https://www.nrel.gov/pv/cell-efficiency.html (accessed 2024-02-22).
- (2) Ma, S.; Yuan, G.; Zhang, Y.; Yang, N.; Li, Y.; Chen, Q. Development of Encapsulation Strategies towards the Commercialization of Perovskite Solar Cells. *Energy Environ. Sci.* **2022**, *15* (1), 13–55. https://doi.org/10.1039/D1EE02882K.
- (3) Emery, Q.; Remec, M.; Paramasivam, G.; Janke, S.; Dagar, J.; Ulbrich, C.; Schlatmann, R.; Stannowski, B.; Unger, E.; Khenkin, M. Encapsulation and Outdoor Testing of Perovskite Solar Cells: Comparing Industrially Relevant Process with a Simplified Lab Procedure. *ACS Appl. Mater. Interfaces* **2022**, *14* (4), 5159–5167. https://doi.org/10.1021/acsami.1c14720.
- (4) Wang, T.; Yang, J.; Cao, Q.; Pu, X.; Li, Y.; Chen, H.; Zhao, J.; Zhang, Y.; Chen, X.; Li, X. Room Temperature Nondestructive Encapsulation via Self-Crosslinked Fluorosilicone

- Polymer Enables Damp Heat-Stable Sustainable Perovskite Solar Cells. *Nat Commun* **2023**, *14* (1), 1342. https://doi.org/10.1038/s41467-023-36918-x.
- (5) Wang, H.; Zhao, Y.; Wang, Z.; Liu, Y.; Zhao, Z.; Xu, G.; Han, T.-H.; Lee, J.-W.; Chen, C.; Bao, D.; Huang, Y.; Duan, Y.; Yang, Y. Hermetic Seal for Perovskite Solar Cells: An Improved Plasma Enhanced Atomic Layer Deposition Encapsulation. *Nano Energy* 2020, 69, 104375. https://doi.org/10.1016/j.nanoen.2019.104375.
- (6) Choi, E. Y.; Kim, J.; Lim, S.; Han, E.; Ho-Baillie, A. W. Y.; Park, N. Enhancing Stability for Organic-Inorganic Perovskite Solar Cells by Atomic Layer Deposited Al₂O₃ Encapsulation. Solar Energy Materials and Solar Cells 2018, 188, 37–45. https://doi.org/10.1016/j.solmat.2018.08.016.
- (7) Asgarimoghaddam, H.; Chen, Q.; Ye, F.; Shahin, A.; Song, B.; Musselman, K. P. Zinc Aluminum Oxide Encapsulation Layers for Perovskite Solar Cells Deposited Using Spatial Atomic Layer Deposition. *Small Methods* 2023, 2300995. https://doi.org/10.1002/smtd.202300995.
- (8) Zhou, J.; Tian, X.; Gao, Y.; Zhang, S.; Zhang, Y.; Liu, Z.; Chen, W. Enhancing the Stability of Perovskite Solar Cells with a Multilayer Thin-Film Barrier. *ACS Appl. Energy Mater*. **2023**, *6* (3), 1413–1421. https://doi.org/10.1021/acsaem.2c03298.
- (9) Wang, Y.; Ahmad, I.; Leung, T.; Lin, J.; Chen, W.; Liu, F.; Ng, A. M. C.; Zhang, Y.; Djurišić, A. B. Encapsulation and Stability Testing of Perovskite Solar Cells for Real Life Applications. ACS Mater. Au 2022, 2 (3), 215–236. https://doi.org/10.1021/acsmaterialsau.1c00045.
- (10) Cheacharoen, R.; Bush, K. A.; Rolston, N.; Harwood, D.; Dauskardt, R. H.; McGehee, M. D. Damp Heat, Temperature Cycling and UV Stress Testing of Encapsulated Perovskite

- Photovoltaic Cells. In 2018 IEEE 7th World Conference on Photovoltaic Energy Conversion (WCPEC) (A Joint Conference of 45th IEEE PVSC, 28th PVSEC & 34th EU PVSEC); IEEE: Waikoloa Village, HI, 2018; pp 3498–3502. https://doi.org/10.1109/PVSC.2018.8547430.
- (11) Cao, M.; Ji, W.; Chao, C.; Li, J.; Dai, F.; Fan, X. Recent Advances in UV-Cured Encapsulation for Stable and Durable Perovskite Solar Cell Devices. *Polymers* **2023**, *15* (19), 3911. https://doi.org/10.3390/polym15193911.
- (12) Lee, Y. I.; Jeon, N. J.; Kim, B. J.; Shim, H.; Yang, T.; Seok, S. I.; Seo, J.; Im, S. G. A Low-Temperature Thin-Film Encapsulation for Enhanced Stability of a Highly Efficient Perovskite Solar Cell. *Advanced Energy Materials* **2018**, *8* (9), 1701928. https://doi.org/10.1002/aenm.201701928.
- (13) Ramos, F. J.; Maindron, T.; Béchu, S.; Rebai, A.; Frégnaux, M.; Bouttemy, M.; Rousset, J.; Schulz, P.; Schneider, N. Versatile Perovskite Solar Cell Encapsulation by Low-Temperature ALD-Al₂O₃ with Long-Term Stability Improvement. *Sustainable Energy Fuels* **2018**, *2* (11), 2468–2479. https://doi.org/10.1039/C8SE00282G.
- (14) Perrotta, A.; Fuentes-Hernandez, C.; Khan, T. M.; Kippelen, B.; Creatore, M.; Graham, S. Near Room-Temperature Direct Encapsulation of Organic Photovoltaics by Plasma-Based Deposition Techniques. *J. Phys. D: Appl. Phys.* 2017, 50 (2), 024003. https://doi.org/10.1088/1361-6463/50/2/024003.
- (15) Cheacharoen, R.; Rolston, N.; Harwood, D.; Bush, K. A.; Dauskardt, R. H.; McGehee, M. D. Design and Understanding of Encapsulated Perovskite Solar Cells to Withstand Temperature Cycling. *Energy Environ. Sci.* 2018, *11* (1), 144–150. https://doi.org/10.1039/C7EE02564E.
- (16) Kempe, M. D.; Miller, D. C.; Wohlgemuth, J. H.; Kurtz, S. R.; Moseley, J. M.; Shah, Q.; Tamizhmani, G.; Sakurai, K.; Inoue, M.; Doi, T.; Masuda, A.; Samuels, S. L.; Vanderpan, C.

- E. A Field Evaluation of the Potential for Creep in Thermoplastic Encapsulant Materials. In 2012 38th IEEE Photovoltaic Specialists Conference; IEEE: Austin, TX, 2012; pp 001871–001876. https://doi.org/10.1109/PVSC.2012.6317958.
- (17) Kim, N.; Han, C.; Lee, J.; Baek, D.; Kim, D. Determination of Moisture Ingress through Various Encapsulants Used in CIGS PV Module under Continuously Varying Environment. In 2012 38th IEEE Photovoltaic Specialists Conference; IEEE: Austin, TX, USA, 2012; pp 000887–000890. https://doi.org/10.1109/PVSC.2012.6317744.
- (18) Peike, C.; Hülsmann, P.; Blüml, M.; Schmid, P.; Weiß, K.-A.; Köhl, M. Impact of Permeation Properties and Backsheet-Encapsulant Interactions on the Reliability of PV Modules. *ISRN Renewable Energy* **2012**, *2012*, 1–5. https://doi.org/10.5402/2012/459731.
- (19) Kempe, M. D.; Panchagade, D.; Reese, M. O.; Dameron, A. A. Modeling Moisture Ingress through Polyisobutylene-based Edge-seals. *Progress in Photovoltaics* **2015**, *23* (5), 570–581. https://doi.org/10.1002/pip.2465.
- (20) Bush, K. A.; Palmstrom, A. F.; Yu, Z. J.; Boccard, M.; Cheacharoen, R.; Mailoa, J. P.; McMeekin, D. P.; Hoye, R. L. Z.; Bailie, C. D.; Leijtens, T.; Peters, I. M.; Minichetti, M. C.; Rolston, N.; Prasanna, R.; Sofia, S.; Harwood, D.; Ma, W.; Moghadam, F.; Snaith, H. J.; Buonassisi, T.; Holman, Z. C.; Bent, S. F.; McGehee, M. D. 23.6%-Efficient Monolithic Perovskite/Silicon Tandem Solar Cells with Improved Stability. *Nat Energy* 2017, 2 (4), 17009. https://doi.org/10.1038/nenergy.2017.9.
- (21) Velilla, E.; Jaramillo, F.; Mora-Seró, I. High-Throughput Analysis of the Ideality Factor to Evaluate the Outdoor Performance of Perovskite Solar Minimodules. *Nat Energy* **2021**, *6* (1), 54–62. https://doi.org/10.1038/s41560-020-00747-9.

- (22) Wang, X.; Huang, G. S.; Wu, J. R.; Nie, Y. J.; He, X. J.; Xiang, K. W. Molecular Motions in Glass-Rubber Transition Region in Polyisobutylene Investigated by Two-Dimensional Correlation Dielectric Relaxation Spectroscopy. *Applied Physics Letters* **2011**, *99* (12), 121902. https://doi.org/10.1063/1.3640479.
- (23) McEachran, M. J.; Trant, J. F.; Sran, I.; De Bruyn, J. R.; Gillies, E. R. Carboxylic Acid-Functionalized Butyl Rubber: Synthesis, Characterization, and Physical Properties. *Ind. Eng. Chem. Res.* **2015**, *54* (17), 4763–4772. https://doi.org/10.1021/acs.iecr.5b00421.
- (24) Kapur, J.; Norwood, J. L.; Cwalina, C. D. Determination of Moisture Ingress Rate through Photovoltaic Encapsulants. In 2013 IEEE 39th Photovoltaic Specialists Conference (PVSC); IEEE: Tampa, FL, USA, 2013; pp 3020–3023. https://doi.org/10.1109/PVSC.2013.6745097.
- (25) Scetta, G.; Ju, J.; Selles, N.; Heuillet, P.; Ciccotti, M.; Creton, C. Strain Induced Strengthening of Soft Thermoplastic Polyurethanes under Cyclic Deformation. *Journal of Polymer Science* **2021**, *59* (8), 685–696. https://doi.org/10.1002/pol.20210060.
- (26) Matteocci, F.; Cinà, L.; Lamanna, E.; Cacovich, S.; Divitini, G.; Midgley, P. A.; Ducati, C.; Di Carlo, A. Encapsulation for Long-Term Stability Enhancement of Perovskite Solar Cells.
 Nano Energy 2016, 30, 162–172. https://doi.org/10.1016/j.nanoen.2016.09.041.
- (27) Dong, Q.; Liu, F.; Wong, M. K.; Tam, H. W.; Djurišić, A. B.; Ng, A.; Surya, C.; Chan, W. K.; Ng, A. M. C. Encapsulation of Perovskite Solar Cells for High Humidity Conditions. *ChemSusChem* 2016, 9 (18), 2597–2603. https://doi.org/10.1002/cssc.201600868.
- (28) Fu, Z.; Xu, M.; Sheng, Y.; Yan, Z.; Meng, J.; Tong, C.; Li, D.; Wan, Z.; Ming, Y.; Mei, A.; Hu, Y.; Rong, Y.; Han, H. Encapsulation of Printable Mesoscopic Perovskite Solar Cells Enables High Temperature and Long-Term Outdoor Stability. *Adv Funct Materials* 2019, 29 (16), 1809129. https://doi.org/10.1002/adfm.201809129.

- (29) Cheacharoen, R.; Boyd, C. C.; Burkhard, G. F.; Leijtens, T.; Raiford, J. A.; Bush, K. A.; Bent, S. F.; McGehee, M. D. Encapsulating Perovskite Solar Cells to Withstand Damp Heat and Thermal Cycling. *Sustainable Energy Fuels* **2018**, *2* (11), 2398–2406. https://doi.org/10.1039/C8SE00250A.
- (30) *IEC 61215-2:2021* | *IEC Webstore*. https://webstore.iec.ch/publication/61350 (accessed 2024-04-12).
- (31) Crystallinity / Degree of Crystallinity. NETZSCH Analyzing and Testing. Leading in Thermal Analysis, Rheology and Fire Testing. https://analyzing-testing.netzsch.com/en-US/training-know-how/glossary/crystallinity-degree-of-crystallinity (accessed 2024-03-14).
- (32) Kościuszko, A.; Marciniak, D.; Sykutera, D. Post-Processing Time Dependence of Shrinkage and Mechanical Properties of Injection-Molded Polypropylene. *Materials* **2021**, *14* (1), 22. https://doi.org/10.3390/ma14010022.
- (33) See Supplemental Material at [], which includes Ref. [34], for additional information about the material synthesis method.
- (34) Xiao, Z.; Wang, D.; Dong, Q.; Wang, Q.; Wei, W.; Dai, J.; Zeng, X.; Huang, J. Unraveling the Hidden Function of a Stabilizer in a Precursor in Improving Hybrid Perovskite Film Morphology for High Efficiency Solar Cells. *Energy & Environmental Science* **2016**, *9* (3), 867–872. https://doi.org/10.1039/C6EE00183A.